ELSEVIER

Materials Science and Engineering B69–70 (2000) 219–226

MATERIALS SCIENCE & ENGINEERING B

www.elsevier.com/locate/mseb

Intrinsic microcrystalline silicon (μc-Si:H) deposited by VHF-GD (very high frequency-glow discharge): a new material for photovoltaics and optoelectronics

A. Shah [a], E. Vallat-Sauvain [a], P. Torres [a], J. Meier [a], U. Kroll [a], C. Hof [a], C. Droz [a], M. Goerlitzer [a], N. Wyrsch [a], M. Vanecek [b,*]

[a] *Institute for Microtechnology (IMT), University of Neuchâtel, CH-2000 Neuchâtel, Switzerland*
[b] *Division of Solid State Physics, Institute of Physics, Academy of Sciences of the Czech Republic, CZ-16200, Prague 6, Czech Republic*

Abstract

The development of μc-Si:H technology and the introduction of intrinsic ⟨i⟩ μc-Si:H as photovotaically active material is retraced. Special emphasis is laid on the use of very high frequency glow discharge as a particularly propitious deposition method for μc-Si:H. Thereby, the use of a gas purifier to reduce oxygen content and obtain intrinsic layers with 'midgap' character is described. Recent results obtained with single-junction μc-Si:H solar cells and a-Si:H/μc-Si:H tandem solar cells are given. The analysis of carrier collection in single-junction μc-Si:H solar cells is undertaken with the variable intensity measurements method. It yields effective mobility × lifetime $(\mu\tau)_{\text{eff}}$ products for the i-layer in p–i–n and n–i–p solar cells in the range 10^{-7}–10^{-6} cm^2 V^{-1}. Similar values have been found for $\mu\tau$-products in individual layers based on photoconductivity and ambipolar diffusion length measurements. Transmission electron microscopy images for μc-Si:H layers are given. They display a complex microstructure not suspected before. On the other hand, atomic force microscopy data reveal a pronounced surface roughness that correlates well with the optical light scattering and with the pronounced enhancement of the apparent optical absorption coefficient, in the 1–2 eV region, as already observed before.

Keywords: Hydrogenated microcrystalline silicon; VHF–GD; Photovoltaic; Thin-film silicon solar cells; Transmission electron microscopy (TEM)

1. Introduction, 'history' of plasma-deposited μc-Si:H

In 1968 Veprek and Marecek [1] succeeded for the first time with the deposition of hydrogenated microcrystalline silicon (μc-Si:H). They used a hydrogen plasma, chemical vapour transport and deposition temperatures of about 600°C. In 1975 Spear and LeComber [2] published results of Chittick and of their own work on the successful doping of the hydrogenated amorphous silicon (a-Si:H) at low temperatures ($\approx$ 200°C) using the plasma-enhanced chemical vapour deposition (PECVD). Then, in 1979, a Japanese group [3], showed that doped μc-Si:H can be deposited (by adding hydrogen as additional process gas) from a high power inductive silane glow discharge. From that time on, many studies have been carried out on the preparation of μc-Si:H by PECVD and on its subsequent characterisation [4]. Amorphous silicon together with hydrogenated microcrystalline silicon attracted much attention as candidates for low cost solar cell fabrication. The high conductivity and high transparency of such doped μc-Si:H encouraged many research groups to substitute it for doped amorphous layers as p-type window layers in a-Si:H p–i–n solar cells [5]. μc-Si:H was also proposed for thin-film transistors TFTs) [6]. Some researchers attempted, with very limited success, to make entirely microcrystalline solar cells. However, in general, intrinsic microcrystalline silicon was for a long time not seriously considered to be of any real use as an active photovoltaic material: It was generally assumed that μc-Si:H is necessarily semiconductor with a high defect density and that it is therefore not usable as a photovoltaically active layer in a solar cell device. The strong n-type character generally observed in as-deposited undoped μc-Si:H was taken as a further indication that μc-Si:H basically has a very high defect density. Still, oxygen contamination was already men-

* Corresponding author. Tel.: +42-2-20318540; fax: +42-2-3123184.

0921-5107/00/$ - see front matter
PII: S0921-5107(99)00299-8

tioned as an alternative explanation for the n-type character [7].

It was also not clear what bandgap should be attributed to μc-Si:H. Indeed, early papers do not mention that μc-Si:H has in reality a gap of 1.12 eV (just like c-Si); this has only been shown in recent publications [8] [9].

A further reason why μc-Si:H was in the beginning not seriously studied for photovoltaic applications, was the long fabrication times that were required for such layers in the case of 'standard' PECVD deposition techniques [10,11]. Typical reported deposition rates were below 1 Å s^{-1}. This means e.g. that at a rate of 1 Å s^{-1} a deposition time of more than 8 h(!) is needed to obtain a typical absorber thickness of 3 μm.

Due to the excellent optoelectronic properties that can be obtained with improved deposition methods (like very high frequency glow discharge (VHF–GD)), μc-Si:H is experiencing a new wave of interest in the scientific community. We are just starting to understand this material with its basic features and varieties. The present paper will give an overview of the known properties related to this 'new' thin-film semiconductor material.

2. Microcrystalline silicon by the VHF–GD technique

Several deposition techniques have been developed so far to fabricate microcrystalline silicon layers [12]. The standard capacitively coupled 13.56 MHz industrial frequency PECVD technique is the commonly used method for thin-film silicon deposition. Due to the effect of plasma, substrate temperatures as low as 200°C can thereby be used for the deposition of microcrystalline silicon. In 1987 the VHF–GD, with a plasma excitation frequency of 70 MHz was introduced, for the first time, by our group [13], both for amorphous and microcrystalline silicon (in the latter case, always with hydrogen diluted silane). Compared to conventional RF plasma deposition at 13.56 MHz excitation frequency, VHF–GD leads to higher deposition rates and, for μc-Si:H, to larger grain sizes [14,15]. Results from plasma diagnostics [16,17] and impedance analysis [18] suggest that a higher electron density, an increased flux of ion bombardment with ions of lower average/peak energy and a higher flow of atomic hydrogen to the surface of the growing layer, all combine (in the case of VHF–GD) to create favourable conditions for the growth of μc-Si:H; further relevant detailed plasma investigations and impedance studies are given in [19,20].

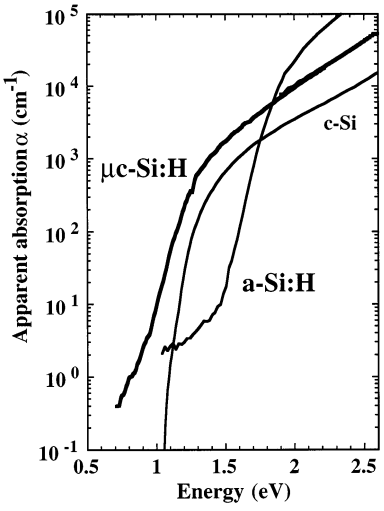

Fig. 1. 'Effective' (or apparent) optical absorption of a μc-Si:H layer deposited by VHF-GD as directly measured by CPM [27] in comparison with amorphous and crystalline silicon.

It turns out that an important condition to obtain photovoltaically active intrinsic μc-Si:H for use in p–i–n or n–i–p type solar cells is to ensure its 'midgap' character (E_F at midgap). This can be achieved either by a delicate compensation technique using boron 'microdoping' [21–23], or, by the silane gas purifier technique introduced by our group [24–26]. The gas purifier reduces oxygen contamination of the feed gas and, thereby, also the oxygen content in the deposited films for both amorphous as well as microcrystalline silicon. Microcrystalline silicon with reduced oxygen content, less than 5×10^{18} cm^{-3}, shows indeed 'midgap' character. The purifier technique simplified the further exploration and progress of microcrystalline silicon as thin-film PV material.

An important property of PV materials is their optical absorption coefficient. Absorption studies reveal that the measured optical absorption of μc-Si:H films grown by VHF is in general higher than that of crystalline silicon. Fig. 1 compares the absorption behaviour of a typical VHF-grown μc-Si:H film with those of amorphous and crystalline silicon. Further analysis and detailed absorption studies have shown that the surface possesses—as deposited—a naturally rough texture which contributes to obtaining an enhanced 'effective' optical absorption in such films [8,9,27]. The actual bandgap of μc-Si:H was thereby confirmed to be about 1.12 eV, i.e. equal to that of crystalline silicon wafers. The apparent shift in bandgap energy towards lower values is, thus, entirely due to the light-scattering effect arising from the rough surface texture of the investigated μc-Si:H layers. One of the main quality parameters of μc-Si:H is the amount of sub-bandgap absorption (at photon energies < 1eV); this value can be correlated with the defect density in the material. From Fig. 1 it can be seen that μc-Si:H layers deposited by VHF–GD can have in the range 0.6–1 eV absorption coefficients that are well below 1 cm^{-1}. This means that their corresponding average defect density is indeed very low.

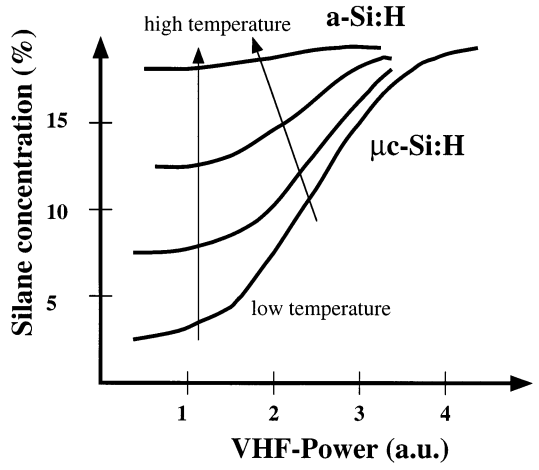

Fig. 2. Rough schematic sketch of different growth regions for amorphous and microcrystalline silicon in the case of VHF–GD.

The region of plasma deposition parameters favourable for the growth of microcrystalline silicon is rather large. Fig. 2 gives an empirical schematic sketch of the corresponding growth regions for μc-Si:H and a-Si:H in function of applied VHF-power and silane concentration.

An important condition to enable the use of μc-Si:H in devices is to increase its deposition rate, whilst still depositing 'high-quality' material. Especially in relation to the production of p–i–n type solar cells, a high deposition rate and a reduction in i-layer thicknesses thanks to optical light-trapping are essential factors. It has been shown that the deposition rate of μc-Si:H can be increased by different ways. As already mentioned, the increase of excitation frequency directly leads to an increase in deposition rate [14,15]. Whilst maintaining VHF-conditions, our group has further observed that the rate can be increased by applying higher input powers. Thus, reasonable μc-Si:H films and cells could be fabricated at 10 Å s^{-1} [28–30]. By applying a combination of the VHF–GD and of the hot-wire deposition techniques, our group even succeeded in obtaining deposition rates up to 26 Å s^{-1} [31]. These results show that there is, in principle, no very restrictive limit for the fast formation of the grains when using glow–discharge deposition techniques. However, much further work has to be done in this field of deposition rate, especially with respect to large-area deposition for the manufacturing of entire solar photovoltaic modules.

A very useful tool for the monitoring of glow discharge plasmas has been found with optical emission spectroscopy (OES) [10,32]. This tool allows one to directly monitor the state of the plasma during the deposition of amorphous or microcrystalline silicon by observing the spectral lines at 414 nm (SiH*) and 656 nm (H_α). Detailed studies for VHF–GD show that the SiH*/H_α-ratio varies with applied power and H_2-dilution ratio; thereby marking the parameter region for obtaining microcrystalline growth [33,34]. OES is therefore a very powerful technique in order to monitor in a production situation, the process windows to be maintained for the growth of device-quality μc-Si:H layers, for solar cells and other devices.

3. Solar cells

The diffusion length of electrons and holes in μc-Si:H are around 1 μm (see Section 4) and are, thus, insufficient to ensure satisfactory collection in devices that are a few μm thick. Thus, one needs to obtain drift-assisted collection of the photogenerated carriers, and therefore uses an intrinsic layer as photovoltaically active layer. In analogy to the case of amorphous silicon cells, one can thereby either use the n–i–p (substrate-type) or the p–i–n (superstrate-type) diode configuration. Our group has followed up both alternatives and has established basic know how for the preparation of p–i–n [21,23,35] as well as of n–i–p [36,37] solar cell devices. These microcrystalline cells show indeed an enhanced spectral response in the infrared region when compared with amorphous silicon: one observes a significant response signal for wavelengths up to about 1100 nm; this is in accordance with the absorption behaviour shown in Fig. 1. Solar cell efficiencies of up to 8.5% ($V_{oc} = 531$ mV, FF = 70%, $J_{sc} = 22.9$ mA cm^{-2}) could be achieved sofar at deposition temperatures of about 220°C. An important advantage of all these microcrystalline silicon solar cells is the absence of any light-induced degradation effect; this is in striking contrast with all amorphous silicon based devices. Similar results have been achieved by other groups [38–40], but partly at considerably higher deposition temperatures of up to approx. 500°C [38]. The low bandgap of μc-Si:H (1.12 eV) opens up the possibility to combine it advantageously, in a tandem solar cell configuration, with amorphous silicon which has a high bandgap (1.7–1.8 eV). These so-called 'Micromorph' (microcrystalline/amorphous silicon) tandem cells consist of a microcrystalline silicon bottom cell and an amorphous silicon top cell. Stabilised micromorph tandem cell efficiencies in the range of 11–12% have been reported sofar [39,41,42].

An interesting novel characterisation method that can be used to analyse complete p–i–n devices is the one based on so-called 'variable intensity measurements' (VIM). In recent work [43] Merten et al. have shown that the recombination losses of a-Si:H p–i–n junctions can be evaluated by the VIM-technique: Thereby, the IV-curves of a solar cell are determined at different intensities (ranging over several orders of magnitude). At an intermediate range of intensities (high enough for the shunt currents to be negligible, but

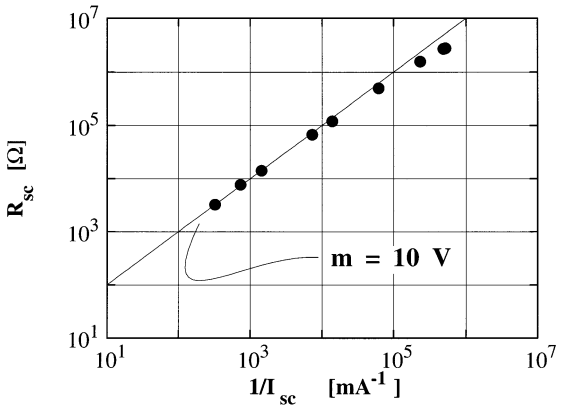

Fig. 3. Typical dependence of the short circuit resistance of a microcrystalline p–i–n solar cell on its inverse short circuit current.

sufficiently low to avoid any series resistance limitation), one observes a linear behaviour of the short circuit resistance R_{sc} vs. the inverse short circuit current, $1/I_{sc}$. Merten et al. have shown that this behaviour can be explained on the basis of an equivalent circuit that takes into account bulk recombination losses. This model can also be extended to analyse μc-Si:H solar cells [44]. Thereby, the proportionality between R_{sc} and $1/I_{sc}$ can be, just as in the case of a-Si:H p–i–n junctions, expressed (in a first approximation) by the formula:

$$R_{sc} = I_{ph}^{-1}.\frac{(\mu\tau)_{eff} V_{bi}^2}{d_i^2} \quad (1)$$

In this equation $(\mu\tau)_{eff}$ stands for an 'effective i-layer $\mu\tau$-product', V_{bi} is the built-in potential, and d_i refers to the i-layer thickness.

Fig. 3 gives experimental data for a typical μc-Si:H solar cell. One notes that in this example the short circuit resistance is proportional to $1/I_{sc}$ over at least two orders of magnitude. Typical values for the slope $m = dR_{sc}dI_{ph}^{-1}$ and corresponding values of $(\mu\tau)_{eff}$ (evaluated according to Eq. (1)) are, furthermore, listed in Table 1.

One generally observes that the values of $(\mu\tau)_{eff}$ obtained for the thicker μc-Si:H cells with the VIM method are in the range 10^{-7}–10^{-6} cm^2 V^{-1} and correspond roughly to the order of magnitude found for the $\mu^0\tau^0$-values measured on individual layers (Section 4).

4. Electronic transport in μc-Si:H layers

So far, the study of electronic transport in μc-Si:H was a rather neglected topic; this was mostly due to the difficulties originally encountered in obtaining truly intrinsic layers. These difficulties have been overcome by the use of the purifier method mentioned above. The approach used in our group for the determination of the transport parameters in μc-Si:H layers has been to apply the well-established a-Si:H characterisation techniques to μc-Si:H, as the latter always contains either a residual amorphous tissue or a structural disorder of some kind (e.g. grain boundaries).

The diffusion length and/or drift length of the free carriers will play a major role in the electrical characteristics of a solar cell device. Both are limited by the band mobility of the carriers μ^0 and the duration of their contribution to a current: under steady-state conditions the latter is defined by us as the recombination time τ^R (by τ^R we mean here the average lifetime of a given carrier before it recombines with a carrier of opposite polarity). Thus, in order to characterise charge transport in μc-Si:H we have used measurement techniques yielding the $\mu^0\tau^R$-products for majority and minority carriers.

As far as the steady-state transport properties of the layers under illumination are concerned, the characterisation techniques used by us are the measurement of photoconductivity (σ_{photo}) and of ambipolar diffusion length L_{amb}; the latter being based on the steady-state photocarrier grating (SSPG) [45] technique. We have observed, when analysing several series of μc-Si:H layers deposited under various conditions (variable plasma power, plasma frequency, and silane concentration) that the $\mu^0\tau^R$ products deduced from the measured values of σ_{photo} and L_{amb} cannot directly be correlated with defect density, structure or oxygen content. It is, thus, difficult to correlate the $\mu^0\tau^R$ products measured on layers with the properties of solar cells.

Table 1
Comparison of 'effective $\mu\tau$-products' $(\mu\tau)_{eff}$ as determined by the VIM-technique in amorphous and in microcrystalline solar cells[a]

i-layer material	i-layer thickness (μm)	$m = dR_{sc}dI_{ph}^{-1}$ (initial) (V)	$(\mu\tau)_{eff}$ cm^2 V^{-1} (initial)	$m = dR_{sc}dI_{ph}^{-1}$ (degraded) (V)	$(\mu\tau)_{eff}$ cm^2 V^{-1} (degraded)
a-Si:H	0.36	30	32.1×10^{-9}	15	16.1×10^{-9}
μc-Si:H	0.8	8	4.2×10^{-8}	–	–
μc-Si:H	3.2	8	67.7×10^{-8}	–	–

[a] The two microcrystalline cells have been deposited in the same process (by partly covering the substrate with a shutter after a quarter of the deposition time) and are, therefore, expected to possess a similar i-layer. The low value of $(\mu\tau)_{eff}$ measured for the 0.8 μm thick μc-Si:H solar cell is probably due to the presence of interface recombination that becomes dominant for collection in this cells.

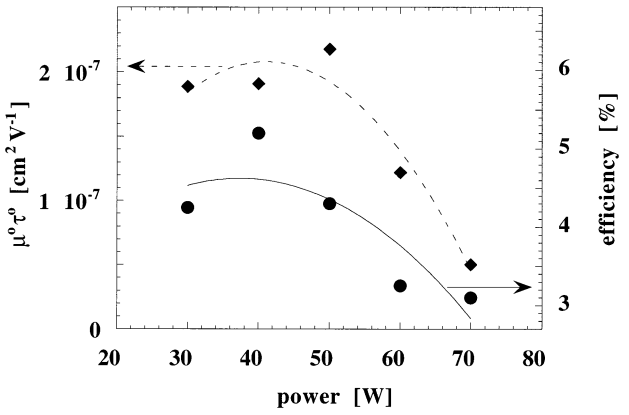

Fig. 4. Correlation between the $\mu^0\tau^0$ product calculated from the values of σ_{photo} and L_{amb} and the efficiency of solar cells with the i-layer deposited in the same conditions as the characterised layers.

However, we have shown that this problem can be eliminated by introducing the parameter b, a method that has already been applied by our group with success to a-Si:H layers [46]. This parameter b, which is defined as $b = \mu_n^0 n_f / \mu_p^0 p_f$, reflects the position of the Fermi level, and is experimentally deduced from σ_{photo} and L_{amb}. Using the parameter b to compare μ-Si:H and a-Si:H layers which have an equivalent free carrier ratio, we can conclude that $\mu^0\tau^R$ products of both majority and minority carriers are in general slightly higher for μ-Si:H layers than for a-Si:H layers.

The variation of $\mu^0\tau^R$ products as a function of b for μc-Si:H shows an *anti*-correlated behaviour of $\mu\tau^R$ products for majority and minority carriers, a behaviour which is identical to that found for a-Si:H. Thus, coplanar measurements of electronic transport under steady-state illumination (i.e. σ_{photo} and L_{amb}) on μ-Si:H layers yield data that is closely similar to that obtained for a-Si:H layers. Based on this observation, we conjecture that the electronic transport model developed for a-Si:H (with amphoteric dangling bonds as recombination centers [47]) should basically also be valid for μc-Si:H. However, this hypothesis must yet be carefully examined, since the transport in solar cells still seems to be different for μc-Si:H when compared to a-Si:H [48].

Nevertheless, we have tentatively assumed that the recombination process is the same in μc-Si:H as in a-Si:H and have introduced also for μc-Si:H the quality parameter $\mu^0\tau^0$, originally defined for a-Si:H [49], as a $\mu\tau$-product that is independent of dangling bond occupation. This quality parameter is, in principle, capable of predicting solar cell behaviour. It is experimentally deduced from σ_{photo} and L_{amb}; the $\mu^0\tau^0$ product is adjusted via the parameter b, which takes into account the position of the Fermi level.

Fig. 4 represents, for a power series of μc-Si:H layers, the values of the $\mu^0\tau^0$ products determined according to [49] when compared with the efficiencies of n–i–p μc-Si:H solar cells incorporating the same layers as i-layers. This first attempt to correlate μc-Si:H layers with solar cells is globally successful and encourages us to continue the application of the $\mu^0\tau^0$ quality parameter also to μc-Si:H.

For a material with a columnar structure and/or crystallographic texture (see Section 5), σ_{ph} and L_{amb}, which are measured in coplanar configuration, basically do not correctly reflect the transport properties relevant to solar cells (transversal transport). Therefore, it is important to characterise electronic transport also in the direction perpendicular to the substrate [37]. However, if one measured the mobility × lifetime ($\mu\tau$) products on μc-Si:H layers with the time of flight (TOF) technique, one observes the same behaviour as that prevailing in a-Si:H [50]. This observation leads one to the hypothesis that the structural anisotropy in these μc-Si:H layers does, in fact, not translate into a significant anisotropy of the electronic transport properties. One notes from TOF measurements that the drift mobility of holes is considerably larger (by almost two orders of magnitude) in μc-Si:H layers than that of a-Si:H layers [37].

5. Microstructure of μc-Si:H layers

The link between μc-Si:H thin-film microstructure and optimal solar cell performance is still far from being elucidated. Indeed, it was so far generally assumed that microcrystalline silicon is constituted either of microcrystallites of a more or less spherical shape embedded in an amorphous tissue, or of another simple microstructure, namely of columnar grains running all the way through the layer, as observed in [51]. The possible effect of an anisotropy in the microstructure, of the grain size and of the grain shape on device performance is still unknown. Transmission electron microscopy (TEM) yields information about the shape, size and crystallographic orientation of crystallites (or grains) in the material, as well as on the presence of cracks and/or of amorphous material at the grain boundaries. These observations can be compared in detail with data evaluated from X-ray diffraction measurements, i.e. with the crystallographic texture as evaluated from the ratio of the peak heights and with the average size of coherent domains (w.r.t. X-ray observation), as calculated from Scherrer's equation.

As stated above, the deposition conditions of μc-Si:H produce films with varying optical and electronic transport properties. A bright field electron micrograph of a sample deposited under conditions close to the amorphous-microcrystalline phase transition are given in Fig. 5. This is one of the simplest microstructures observed for μc-Si:H.

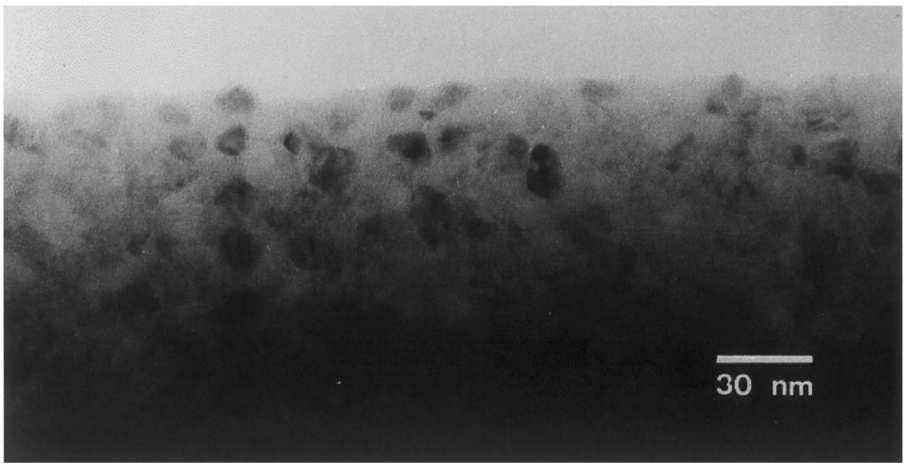

Fig. 5. Plane view bright field micrograph of a sample prepared at a silane concentration close to the amorphous-microcrystalline transition regime. It exhibits small crystallites (7–10 nm diameter) embedded in an amorphous matrix.

From optical measurements [52], one knows that this particular sample has an absorption curve that lies between the absorption curves for microcrystalline and for amorphous silicon. From our TEM picture, we can roughly estimate that the crystalline volume fraction is about 50%. Despite this, only a very faint X-ray signal indicative of crystallinity was observed for this sample. Thus, optical measurements and TEM micrographs are more sensitive to the amorphous fraction than X-ray measurements.

Fig. 6 shows a much more complex microstructure observed in a sample grown with 2.5% silane in hydrogen [52]. We can observe grains pointing out of the surface, resulting in a rough sample to air interface. A characteristic feature observed in this sample are leaflike grains pointing out of the sample. These are rather large monocrystals (150 nm diameter, 350 nm long) with a central symmetry axis consisting of a stacking fault. A surprisingly similar microstructure had already been observed in different thermally recrystallized amorphous silicon samples for TFT applications [53]. This microstructure results from a specific growth mechanism: dendritic growth has been suggested in [53] for the thermally recrystallised samples, but whether the growth mechanism is the same for direct plasma deposition. X-ray diffraction spectra of this sample revealed a strong 'crystallographic texture', which may be defined simply as a condition in which the crystallites orientation in non-random. In this sample, the $\langle 220 \rangle$ direction is the preferred growth direction. A preferred $\langle 220 \rangle$ orientation means that, in most of the crystallites, the (220) planes are parallel to the sample surface, i.e. the growth of the crystallites occurs by piling up (220) planes. Until now, the detailed mechanism of textured growth in the hydrogen-rich plasma remains unclear and needs further investigations. The natural, as-grown surface roughness of this sample has been determined by Atomic Force Microscopy to have a root mean square roughness Sq = 18 nm; such a rough surface leads to strong optical light scattering. This effect is of great practical importance when the layer is incorporated into a solar cell as it results in an enhanced light trapping, and thus leads to an increased short-circuit current. It is yet not quite clear how far the microstructure of the intrinsic layer actually incorporated into the p–i–n solar cell (i.e. deposited on an underlying microcrystalline p-layer) at these dilution levels is comparable with the microstructure of the individual layers presented here, i.e. of layers deposited directly on glass. Neither is the microstructure known for i-layers incorporated into n–i–p solar cells (i.e. deposited on an underlying microcrystalline n-layer).

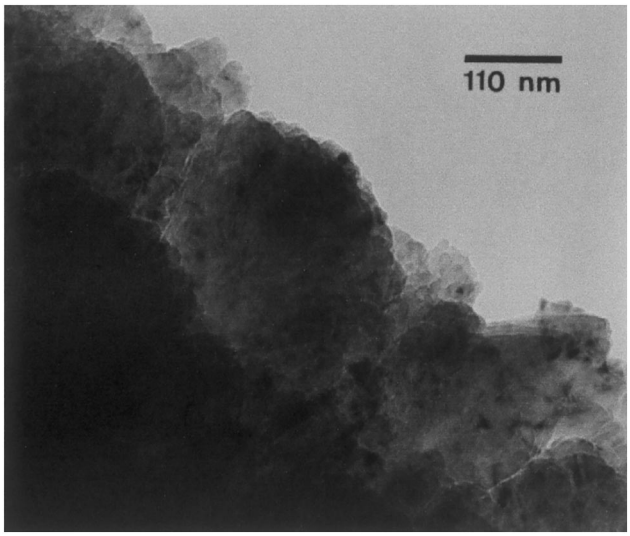

Fig. 6. Cross-section bright field micrograph of μc-Si:H layer exhibiting a complex microstructure.

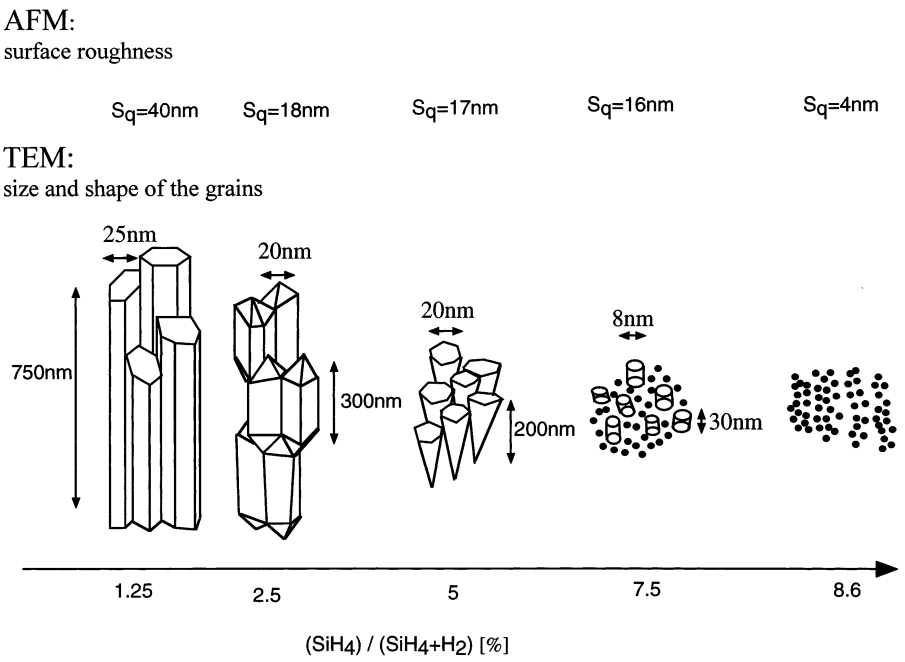

Fig. 7. Schematic evolution of the microstructure of samples in a dilution series.

Crystallite grain size can be estimated from the broadening of the X-ray diffraction peaks using the Debye–Scherrer equation. In this model, a decreasing grain size leads to an increasing peak width. Typically, the grain size calculated for the sample presented in Fig. 6 varies from 24 to 12 nm depending one the hkl-reflection used for the calculation. One can indeed typically observe such small grains in the TEM micrograph (Fig. 6). But larger features (length of the grains) have sizes of the order of 100 nm. The upper limit for size determination with the Debye–Scherrer equation is of the order of 100–200 nm. The X-ray peak broadening will, thus, be insensitive to variations of the larger-scale microstructure. We can conclude that although X-ray diffraction measurements give here useful information on the presence of crystallinity and texture, the grain size value evaluated from the peak broadening in X-ray diffractometry by the Scherrer's method is misleading with respect to the evolution of the size of the largest microstructural features.

The variety of microstructures observed in our μc-Si:H layers deposited on glass can be summarised in Fig. 7.

6. Conclusions and outlook

Intrinsic microcrystalline silicon deposited at temperatures as low as 200–250°C by the VHF–GD method has been used successfully as photovoltaically active material within p–i–n and n–i–p type solar cells. Thereby, the spectral response of such cells has been extended into the near-infrared region. This opens up the possibility of interesting microcrystalline/amorphous (so-called 'micromorph') silicon tandem solar cells; these solar cells have the potential to extend the efficiency range for low-cost, low temperature thin-film silicon solar cells. Of course the same type of p–i–n or n–i–p diodes can also be used as thin-film photosensors, once again with an enhanced near-infrared detection capacity. In order to optimise further these devices, detailed investigations into the correlation between device collection, electronic transport properties and microstructure are needed. Such work has just started; the first results obtained by our group are reported here: they show a striking similarity between electronic transport in amorphous and microcrystalline silicon, but a pronounced difference in the microstructure. This observation clearly calls for in-depth further research. It is reasonable to expect that further understanding of material's properties will permit one to obtain solar cells with even higher efficiencies (e.g. micromorph tandem solar cells with hopefully around 15% stable efficiency), improved photosensors and also other thin-film electronic devices.

Acknowledgements

This work was supported by the Swiss Federal Office of Energy BFE/OFEN No. 19431 and the Swiss National Science Fund under grant FN52337.

References

[1] S. Veprek, V. Marecek, Sol. St. Elec. 11 (1968) 683.
[2] W.E. Spear, P.G. LeComber, Sol. State Comm. 17 (1975) 1193.
[3] S. Usui, M. Kikuchi, J. Non.-Cryst. Sol. 34 (1979) 1.
[4] G. Willeke, in: J. Kanicki (Ed.), Amorphous and Microcrystalline Semiconductor Devices: Materials and Device Physics, Artech House, Norwood, 1992.
[5] J. Yang, et al., Proceedings of the 1st WCPEC, 1994, p. 380.
[6] S.S. He, M.J. Wiliams, D.J. Stephens, G. Lucovsky, J. Non-Cryst. Sol. 164-166 (1993) 731.
[7] G. Lucovsky, C. Wang, M.J. Williams, Y.L. Chen, D.M. Maher, Proc. Mat. Res. Soc. Symp. 283 (1993) 443.
[8] A. Poruba, et al., Proceedings of the 14th EPVSEC, 1997, p. 2105.
[9] M. Vanecek, N. Beck, A. Poruba, Z. Remes, M. Nesladek, J. Non-Cryst. Solids 227 (1998) 967.
[10] A. Matsuda, J. Non-Cryst. Solids 59 (1983) 767.
[11] P.G. LeComber, J. Non-Cryst. Solids 59 (1983) 795.
[12] W. Luft, Y.S. Tsuo, Hydrogenated Amorphous Silicon Alloy Deposition Processes, Marcel Dekker, New York, 1993.
[13] H. Curtins, N. Wyrsch, A. Shah, Electron. Lett. 23 (1987) 223.
[14] F. Finger, P. Hapke, M. Luysberg, R. Carius, H. Wagner, Appl. Phys. Lett. 65 (1994) 2588.
[15] R. Flückiger, et al., Proc. Mat. Res. Soc. Symp. 358 (1995) 751.
[16] A. Howling, J.-L. Dorier, C. Hollenstein, U. Kroll, F. Finger, J. Vac. Sci Technol. B 10 (1992) 1080.
[17] M. Heintze, R. Zedlitz, G.H. Bauer, J. Phys. D Appl. Phys. 26 (1993) 1781.
[18] U. Kroll, Y. Ziegler, J. Meier, H. Keppner, A. Shah, Proc. Mat. Res. Soc. Symp. 336 (1994) 115.
[19] U. Kroll, Ph. D. thesis, University of Neuchâtel, 1994.
[20] H. Keppner, U. Kroll, J. Meier, A. Shah, Solid State Phenomena 44-46 (1995) 97.
[21] J. Meier, R. Flückiger, H. Keppner, A. Shah, Appl. Phys. Lett. 65 (1994) 860.
[22] R. Flückiger, J. Meier, M. Goetz, A. Shah, J. Appl. Phys. 77 (1995) 712.
[23] J. Meier, et al., Proc. Mat. Res. Soc. Symp. 420 (1996) 3.
[24] P. Torres, et al., Appl. Phys. Lett. 69 (1996) 1373.
[25] U. Kroll, et al., J. Vac. Sci. Technol. A 13 (1995) 2742.
[26] U. Kroll, et al., Proc. Mat. Res. Soc. Symp. 377 (1995) 39.
[27] N. Beck, et al., Proc. Mat. Res. Soc. Symp. 452 (1997) 761.
[28] P. Torres, et al., Proc. Mat. Res. Soc. Symp. 452 (1997) 883.
[29] P. Torres, et al., Physica Status Solidi; Rapid Research Notes, 1997.
[30] P. Torres, et al., Proceedings of the IEEE PVSC, 1997, p. 711.
[31] J. Meier, et al., Proceedings of the 2nd WCPVSEC, 1998, p. 375.
[32] Y. Mishima, S. Miyazaki, M. Hirose, Y. Osaka, Phil. Mag. B 46 (1982) 1.
[33] P. Torres, H. Keppner, H. Meier, Proceedings of the 5th European Conference on Thermal Plasma Processes, 1998.
[34] P. Torres, Ph. D. thesis, University of Neuchâtel, 1999.
[35] J. Meier, et al., Proc. Mat. Res. Soc. Symp. 507 (1998) 139.
[36] M. Goetz, et al., Proc. Mat. Res. Soc. Symp. 452 (1997) 877.
[37] N. Wyrsch, et al., Proceedings of the 2nd WCPVSEC, 1998, p. 467.
[38] K. Yamamoto, et al., Proc. Mat. Res. Soc. Symp. 507 (1998) 131.
[39] K. Saito, et al., Proceedings of the 2nd WCPVSEC, 1998, p. 351.
[40] O. Kluth et al., Proc. Mat. Res. Soc. Symp. (1999).
[41] J. Meier, et al., J. Non-Cryst. Solids 227–230 (1998) 1250.
[42] K. Yamamoto, T. Suzuki, M. Yoshimi, A. Nakajima, Proceedings of the 14th EPVSEC, 1997, p. 1018.
[43] J. Merten, et al., Proceedings of the 14th EPVSEC, 1997, p. 1424.
[44] J. Merten, et al., IEEE Trans. Elec. Dev. 45 (1998) 423.
[45] D. Ritter, K. Weiser, E. Zeldov, J. Appl. Phys. 62 (1987) 4563.
[46] A. Shah, Phil. Mag. B 75 (1997) 925.
[47] J. Hubin, A. Shah, E. Sauvain, Phil. Mag. Lett. 66 (1992) 115.
[48] N. Wyrsch, N. Beck, J. Meier, P. Torres, A. Shah, Proc. Mat. Res. Soc. Symp. (1998) 181.
[49] N. Beck, N. Wyrsch, C. Hof, A. Shah, J. Appl. Phys. 79 (1996) 9361.
[50] N. Beck, N. Wyrsch, E. Sauvain, A. Shah, Proc. Mat. Res. Soc. Symp. 297 (1993) 479.
[51] F. Finger, et al., Proc. Mat. Res. Soc. Symp. 452 (1997) 725.
[52] U. Kroll, J. Meier, A. Shah, S. Mikhailov, J. Weber, J. Appl. Phys. 80 (1996) 4971.
[53] M.K. Hatalis, D.W. Greve, J. Appl. Phys. 63 (1988) 2260.